We are IntechOpen, the world's leading publisher of Open Access books
Built by scientists, for scientists

6,900
Open access books available

185,000
International authors and editors

200M
Downloads

154
Countries delivered to

Our authors are among the

TOP 1%
most cited scientists

12.2%
Contributors from top 500 universities

BOOK CITATION INDEX
CLARIVATE ANALYTICS
INDEXED

WEB OF SCIENCE™

Selection of our books indexed in the Book Citation Index
in Web of Science™ Core Collection (BKCI)

Interested in publishing with us?
Contact book.department@intechopen.com

Numbers displayed above are based on latest data collected.
For more information visit www.intechopen.com

Hybrid-Powered Autonomous Robots for Reducing Both Fuel Consumption and Pollution in Precision Agriculture Tasks

Mariano Gonzalez-de-Soto, Luis Emmi and
Pablo Gonzalez-de-Santos

Additional information is available at the end of the chapter

Abstract

Environmental contamination and the resulting climate change are major concerns worldwide. Agricultural vehicles that use fossil fuels emit significant amounts of atmospheric pollutants. Thus, this study investigates techniques to reduce fuel consumption in robotic vehicles used for agricultural tasks and therefore reduce atmospheric emissions from these automated systems. A hybrid energy system for autonomous robots devoted to weed and pest control in agriculture is modeled and evaluated, and its exhaust emissions are compared with those of an internal combustion engine-powered system. Agricultural implements require power for hydraulic pumps and fans; this energy is conventionally provided by power take-off (PTO) systems, which waste substantial amounts of energy. In this work, we examine a solution by designing and assessing a hybrid energy system that omits the alternators from the original vehicle and modifies the agricultural implements to replace the PTO power with electrical power. The hybrid energy system uses the original combustion engine of the tractor in combination with a new electrical energy system based on a hydrogen fuel cell. We analyze and compare the exhaust gases resulting from the use of (1) an internal combustion engine as the single power source and (2) the hybrid energy system. The results demonstrate that the hybrid energy system reduced emissions by up to approximately 50%.

Keywords: atmospheric emissions, exhaust gases, hybrid power, robotic vehicles, precision agriculture

1. Introduction

Off-road vehicles based on internal combustion engines use large amounts of fossil fuels that emit large amounts of pollution into the atmosphere. According to the US Environmental Protection Agency (EPA) [1], internal combustion engines emit carbon dioxide (CO_2), nitrogen oxide (NO_x), carbon monoxide (CO), particulate matter and hydrocarbons. CO_2 and NO_x are greenhouse gases that contribute to global warming, whereas sulfur dioxide (SO_2) and NO_x emissions contribute to acid rain. Therefore, the use of internal combustion engines is a major environmental concern. Furthermore, these chemical compounds also cause health problems. For example, NO_x may cause respiratory diseases and intensify existing heart disease; CO can reduce oxygen delivery to the body's tissues and organs, which reduces an individual's work capacity, mental skills and learning ability. Hydrocarbons are volatile organic compounds that can cause headaches, dizziness, and loss of consciousness, among other effects. Moreover, some of these substances, such as benzene, are carcinogenic and increase the likelihood of leukemia. Particle matter emitted from combustion engines (nitrates, sulfates, organic chemicals, metals, and dust particles) can also affect lung and heart functions, causing serious health problems.

Many efforts to mitigate these negative effects have conducted analyses of energy use and the pollution emitted by agricultural tractors. In the early 2000s, several research studies compared different methods and calculated the average absolute and specific emission values from agricultural tractors, concluding that the use of hydrocarbon fuels must be progressively replaced by cleaner fuels or electrical systems [2]. Other studies have proposed using a model of fossil fuel to simulate possible agricultural production scenarios to improve future techniques [3]. In recent years, researchers have analyzed how increasing the soil organic carbon content decreases the draft force in plowing, resulting in reduced fuel consumption and emissions [4].

Several studies have analyzed the exhaust gas emissions from internal combustion engines in the last two decades, and many such studies have focused on agricultural machines. For example, a mathematical model of a tractor was developed in [5] to analyze the fuel consumption and engine emissions for different engine control strategies and engine transmission characteristics, whereas in [6], the exhaust emissions and fuel composition of a real tractor during plowing were measured and correlated to the load factor of the tractor. These works concluded that fuel consumption and emissions depend on the engine speed and load conditions.

Many studies have analyzed the impact of alternative energy sources such as biofuels and have demonstrated that biofuels can benefit the environment and society [7]. However, many of these studies have proposed the use of batteries and have examined various battery technologies available for use in solar-assisted plug-in hybrid electrical tractors that can be used in light-duty agricultural operations [8]. These researchers have also conducted life cycle analyses of a solar-assisted plug-in hybrid electrical tractor and compared the results with that of a similar power output internal combustion engine tractor considering both economic costs and environmental emissions; they determined that the life cycle costs of solar-assisted plug-in hybrid electrical tractors are lower than those of internal combustion engines.

Another important alternative to batteries is fuel cells. For example, several researchers have proposed the use of environmentally benign fuel cells for power production in field crop

production and distribution and presented engineering systems analyses of how such systems can reduce pollution [9]. Others have compared the theoretical maximum efficiencies of a fuel cell and a Carnot cycle using the same fuel to determine the net reaction [10]. They found that the maximum efficiencies of both systems are similar, but in practice, a fuel cell is more efficient because internal combustion engines cannot operate at their theoretical maximum efficiency. Other researchers have compared battery electrical vehicles, hydrogen fuel cell electrical vehicles and hydrogen fuel cell plug-in hybrid vehicles [11]. These researchers determined that battery electrical vehicles and hydrogen fuel cell plug-in hybrid vehicles have similar life cycle costs. The life cycle costs of these vehicles are higher than the costs of internal combustion engines but could decrease by 2030.

The approach presented in this work originated from the observation that during precision agriculture tasks with robotized vehicles, the internal combustion engine frequently supplied more power than needed, particularly when the implement (a tool or utensil for performing agricultural work) used a power take-off (PTO) device as a power source. Thus, the objective of this work was to develop, implement and assess a hybrid energy system for agricultural robotic vehicles. The proposed energy system combines the use of batteries, a hydrogen fuel cell and photovoltaic cells with the original internal combustion engine of the tractor to achieve a substantial decrease in fossil fuel use, reducing the pollutant emissions.

The rest of this work is organized as follows. In Section 2, the autonomous robot and agricultural implements used in this study are described. In Section 3, a path planning method for reducing the fuel consumption is presented. Then, in Section 4, the energy demanded in the selected agricultural tasks is analyzed, and the hybrid energy system designed to reduce the system energy consumption is described. Section 5 studies the energy requirements of the selected agricultural tasks and the required features of the hybrid energy system. Finally, the main results are discussed in Section 6, and the main conclusions are summarized in Section 7.

2. Systems description

The energetic model derived in this work was tested in a system composed of an autonomous robot and three different implements, each designed for a different agricultural task. The autonomous robot consisted of several subsystems:

- A central controller

- An internal combustion engine

- A hydrogen fuel cell

- A photovoltaic panel

- A set of batteries

- An energy management system

- A fuel consumption measurement system used to estimate the exhaust gases from the internal combustion engine

These subsystems and the implements are described below. The modifications made to the implements such that the power provided by the PTO device could be replaced with electrical power are also described, and the implement power features needed to design the energy model are detailed.
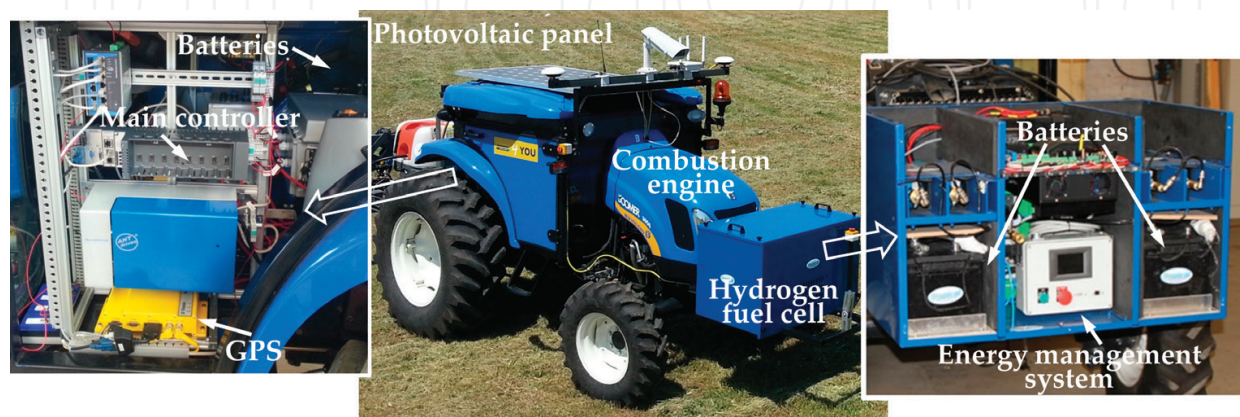
2.1. Autonomous robot

The autonomous robot was based on the commercial CNHi Boomer 3050 CVT tractor (CNHi, Zedelgem, Bruges, Belgium). This vehicle, with a weight of approximately 1700 kg and a gross power of approximately 33.6 kW, was mechanically, electrically and hydraulically modified. The robot power system, originally based on the tractor internal combustion engine, was improved with an additional electrical energy system consisting of (1) a photovoltaic panel, (2) a hydrogen fuel cell and (3) a set of batteries.

A main controller onboard the vehicle managed the main vehicle functions and a safety system that provided safety to the vehicle, the environment and, most importantly, any individuals nearby [12]. The final autonomous robot and the different subsystems attached to it, whose main features are detailed in the following sections, are depicted in **Figure 1**. The size, justification and assessment of the added electrical energy system are presented in Section 5.2.
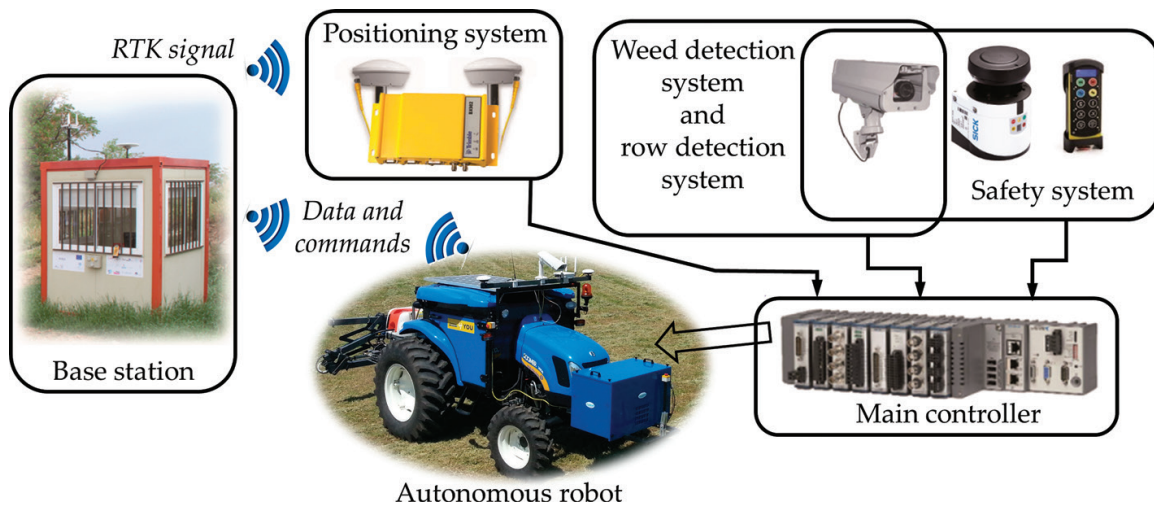
2.1.1. Autonomous robot controller

The autonomous robot controller (see **Figure 2**) allowed the robot to apply an effective treatment with high precision. The autonomous robot controller is based on a hybrid architecture that relies on the main controller based on a CompactRIO-9082 (National Instruments Corporation) running a LabVIEW Real-Time operating system. The controller synchronized and processed the information received from different sensors and the external operator and selected the best behavior for the entire system depending on the current working situation, the perceived environment and the general mission requirements. The controller also communicated with every other subsystem via diverse communication protocols (Ethernet, serial and CAN bus) [13, 14]. The set of these systems (controllers, sensors and actuators) had an average power demand of approximately 170 W for 12-V devices and approximately 260 W for 24-V devices.

Figure 1. Autonomous robot.

Figure 2. Main components of the autonomous robot controller.

The autonomous robot is equipped with a positioning system that consists of a global positioning system (GPS) receiver (Trimble Model BX982), with two antennas to measure the robot's heading with triangulation techniques. The system uses a real-time kinematic (RTK) signal correction provided by a GPS base station located next to the working field. The positioning system provides a location accuracy of approximately ±0.025 m.

A vision system installed onboard the robot was used by

- the weed detection system, which is responsible for detecting weed patches

- the crop row detection system, which is responsible for detecting the rows as a reference for guiding the autonomous robot

- the safety system, which comprised (1) an obstacle detection system based on the robot camera, (2) a laser and (3) a remote controller used by the operator.

A base station generated the mission, which consisted of a plan that defined the trajectories of the robot and a plan for managing the implements, both plans depended on the specific application. After generating the mission, the base station sent both plans to the robot controller and executed them. When the robot was working, the base station was responsible for supervising the status of both the robot and implement in real time and detecting malfunctions, such as service disruptions, incorrect working speeds, incorrect implement statuses and the probability of collisions [15].
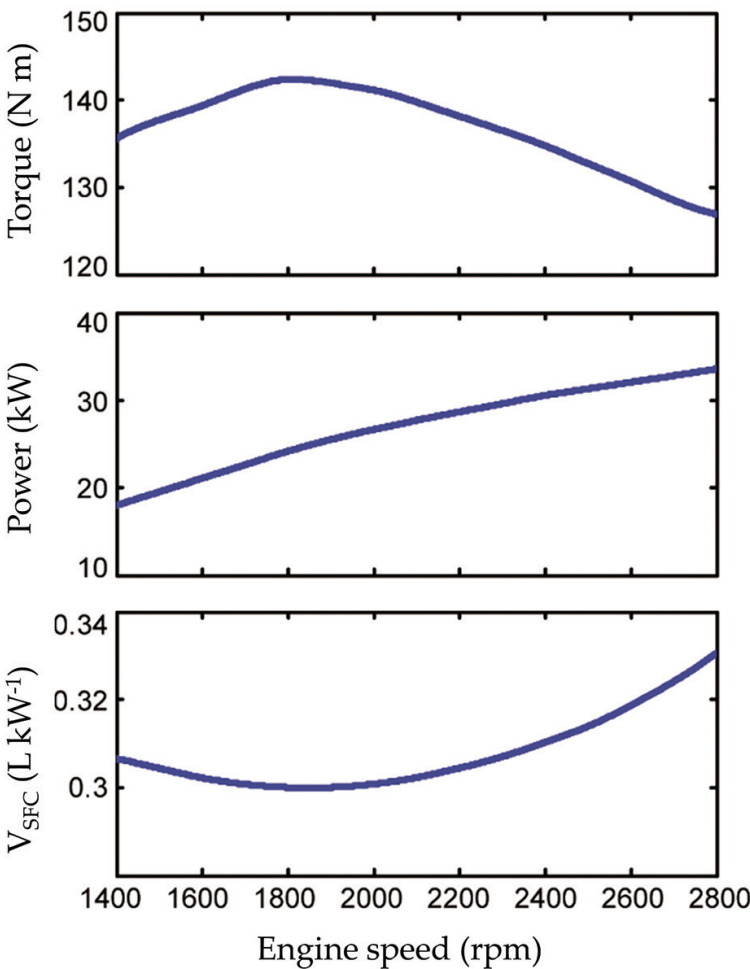
2.1.2. Internal combustion engine

The internal combustion engine can work in two ways:

- As the only power source providing the total power demanded by the agricultural task.

- As a part of the hybrid energy system, providing only a sufficient amount of power to move the autonomous robot with its implement.

The engine was similar to that of the original tractor; however, the maximum ground speed was limited to 7 km h^{-1} for safety reasons. **Figure 3** shows the performance curves of the internal combustion engine provided by the manufacturer, which were used to calculate the exhaust gas emissions and implement the energy demand model. The torque, power curve and specific fuel consumption volume (V_{SFC}) are shown as functions of the engine speed.

2.1.3. Hydrogen fuel cell

A hydrogen fuel cell was used because this device generates electrical power with high performance and can be rapidly refueled. The cell was attached to the front of the robot in a box containing the hydrogen tanks (see **Figure 1**). A proton exchange membrane fuel cell and metal hydride tanks were selected, which provided a power range from 0.5 to 5 kW with a specific hydrogen consumption of approximately 0.74 Nm^3 kW h^{-1}. This value was used to estimate the hydrogen consumption [17]. Nm^3 denotes normal cubic meters, the volume of gas measured under the normal conditions of 0°C and 1.01325 × 10^5 Pa (1 atm) of pressure.

Figure 3. Performance curves of the internal combustion engine [16].

2.1.4. Photovoltaic panel

The photovoltaic panel was used as an additional system for fossil-free energy. This device charged the batteries whenever there was sufficient light, even when the robot was in a garage. The panel was situated on top of the robot to minimize shadows. Only the antennas and camera were attached higher on the robot to improve the signal transmission and camera vision. The panel was set horizontally to collect solar power independent of the orientation (see **Figure 1**).

2.1.5. Batteries

A set of batteries were used to

- store excess electrical energy

- supply energy during periods of high demand, for example, the startup of the internal combustion engine

- ensure that the robot's energy management system had a continuous energy supply.

Because the set of batteries was heavy, one group of batteries was placed over the rear vehicle shaft to reduce the slippage in tasks requiring draft forces. Another battery bank was placed inside the fuel cell box in front part of the tractor and acted as a counterweight, when heavy implements were used (see **Figure 1**).

2.1.6. Energy management system

The energy management system consisted of a controller to manage the electrical energy flow from the hydrogen fuel cell and the photovoltaic panel. This system was responsible for regulating and adapting the electrical power and supervising the electrical energy storage. To accomplish this task, the system collected data about the status of the batteries and hydrogen tanks and controlled the power provided by the hydrogen fuel cell.

2.1.7. Fuel consumption measurement system and model

Fuel consumption was measured using two flowmeters installed in the fuel supply line and return line (see **Figure 4**). The instantaneous fuel consumption was measured as the difference between the data from flowmeter 1 and the data from flowmeter 2.

The flow sensors must be placed behind a fuel filter for protection; therefore, the return line flowmeter must be installed in the pipe between the injectors and the junction with the fuel filter return line. The other flowmeter can be installed between the fuel filter and lift pump or between the lift pump and injection pump. The best position is behind the lift pump; otherwise, low pressure can lead to additional problems resulting from small air bubbles in the sensor circuit. Additionally, a cooling device was added in the return line before flowmeter 2 because a substantial amount of noise was observed in the flowmeter 2 data as a result of the high temperature of the fuel returned by the robot engine.
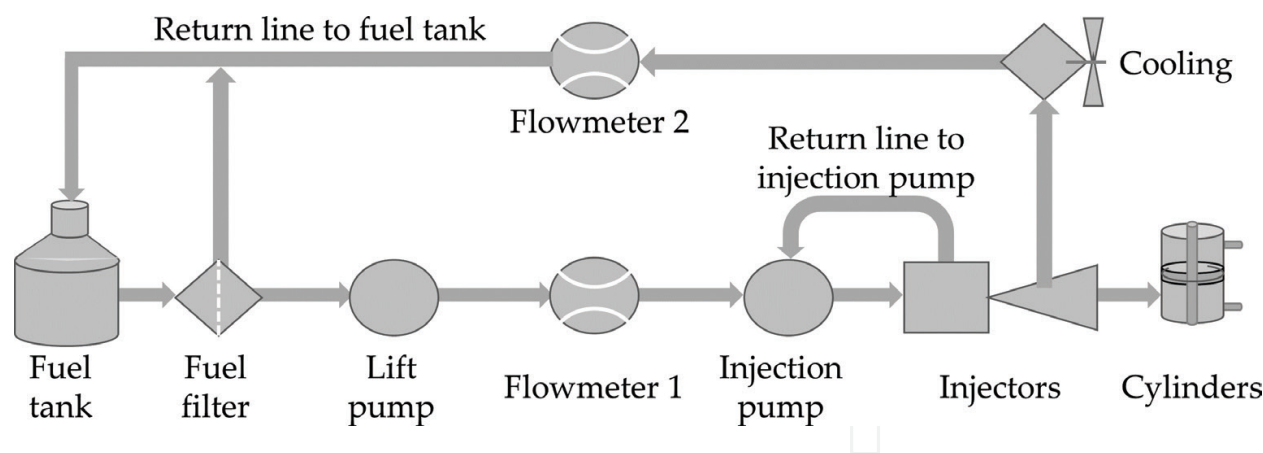
Figure 4. Scheme of the fuel flow system.

These flowmeters must be suitable for measuring diesel fuel and support the robot fuel circuit conditions. According to the characteristics of the fuel system (see **Table 1**), the flowmeters do not need to support high pressures; the nominal flow must be approximately 12.54 L h^{-1}, with a maximum flow of approximately 30 L h^{-1}, which is adequate for oil with a low kinematic viscosity. Furthermore, the flowmeter must deliver a measure of the temperature of the fluid, and the return line flow sensor must be sensitive to a low flow rate.

An effective flowmeter for these applications was a small positive displacement oval gear flowmeter. The oval gear design ensures that the pressure loss across the sensor is very low (less than 1.5×10^4 Pa at full flow) and that the performance remains nearly constant over the entire temperature and viscosity range. The PD400 flowmeter from Titan Enterprises Ltd. (Sherborne Dorset, England, UK) was selected (see **Figure 5**) for both flow lines. **Table 2** presents the main features of the PD400 flowmeter, which has a small, oval, tooth-wheeled counter in addition to an easily replaceable filter that protects the sensor from any floating particles. The flowmeter accuracy was approximately ±2.5% with a low pressure loss of 10^4 Pa [20], and its recommended working temperature range was from 0 to 60°C, which was slightly lower than the temperature of the fluid in the return line; thus, the return line required a small radiator to cool the returned fuel. This fuel consumption measurement system was properly calibrated and validated experimentally. Considering the flowmeter accuracy and the rate of flow in the fuel line, we obtained an accuracy of approximately 0.3 L h^{-1}.

Feature	Value
Lift pump rated flow	12.54 L h^{-1}
Lift pump working pressure	(0.2 ± 0.05) 105 Pa
Maximum flow	~30 L h^{-1}
Density at 15°C	820–845 kg m^{-3}
Gross calorific value	10.40–10.72 kWh L^{-1}
Net calorific value	9.881–10.182 kWh L^{-1}
CO_2 emissions	2.616–2.696 kg L^{-1}

Table 1. Main characteristics of the fuel and fuel systems [16, 18, 19].
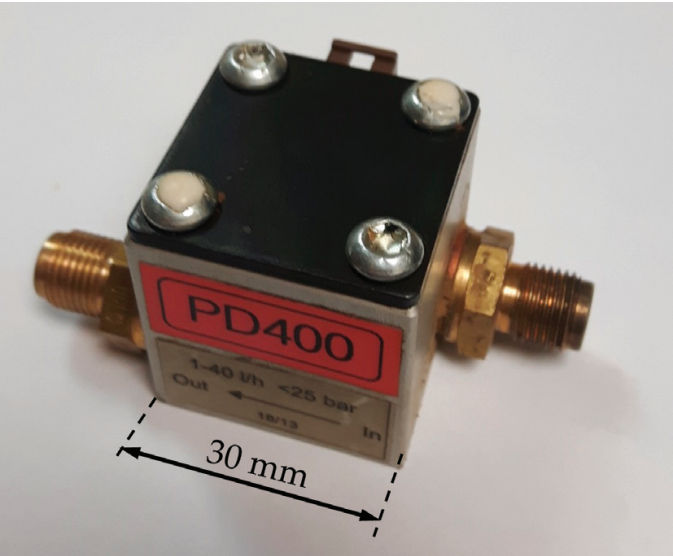
Figure 5. PD400 flowmeter.

Several mathematical models for tractor engine consumption have been proposed in the last few decades; these models show the interest in minimizing fuel consumption in agriculture tasks [21, 22]. In this study, fuel consumption was assumed to depend on the terrain surface and slope, engine speed, throttle position and load conditions, tractor drive type, total weight, drawbar, PTO, and hydraulic and electrical power. To estimate the individual contribution of these elements to fuel consumption, their relationships with energy expenditures must be examined. These relationships were based on estimates using standards, engineering practices, and data suggested by the American Society of Agricultural Engineers (ASAE) [24].

The total energy and fuel consumption can be related through the specific fuel consumption volume, V_{SFC}, which is the fuel volume consumed per power provided, by computing the total fuel consumed, V_{TFC}, as follows:

$$V_{TFC} = \int_0^T V_{SFC}(t) \, \mathrm{P}_{T\_PTOeq}(t)dt \tag{1}$$

where P_{T_PTOeq} is the total equivalent PTO demanded power.

According to ASAE [24], the specific fuel consumption volume can be computed by

Feature	Value
Flow rate	1–60 L h^{-1}
Maximum working pressure	25,105 Pa
K factor	1830 pulses L^{-1}
Temperature range	0–60°C
Accuracy	±2.5% (at a density of 830 kg m^{-3})

Table 2. Main characteristics of the PD400 flowmeter [23].

$$V_{SFC}(t) = \left(0.22 + 0.096 \frac{P_{PTOrated}(t)}{P_{PTOeq}(t)} \right)\left(1 - \left(\frac{n_{PT}}{n_{FT}} - 1 \right)\left(0.45 \frac{P_{PTOeq}(t)}{P_{PTOrated}(t)} - 0.877 \right) \right) \tag{2}$$

and the total equivalent PTO demanded power is given by

$$P_{T\_PTOeq}(t) = \frac{D(t)\,v(t)}{E_T} + \frac{F_{MR}\,v}{Em} + P_{PTO} + P_{hyd} + P_{el} \tag{3}$$

where P_{PTOeq} is the equivalent PTO power; $P_{PTOrated}$ is the rated PTO power; n_{PT} and n_{FT} are the partial and full throttle engine speed, respectively; D is the implement draft force; F_{MR} is the motion resistance (i.e., the difference between the gross traction and net traction; v is the vehicle speed; E_T is the traction efficiency; E_M is the mechanical efficiency of the power transmission from the net flywheel to the PTO; and P_{PTO}, P_{hyd} and P_{el} are the power requirements from the PTO, the hydraulic power and the electrical power, respectively. Details about the model's derivation are provided in [25].

2.1.8. Calculation of the exhaust gas emissions

The exhaust gas emissions were computed by considering the partial load and speed of the engine for a particular work regime according to the ISO 8178 standard [26] and the fuel features specified in [18]. To calculate the partial load, the values of wheel slippage (the difference between the ground speed provided by GPS and the wheel speed provided by the control system), PTO speed, engine speed, three-point hitch position (which determines the plowing depth when the cultivator is used), and terrain slope (obtained from the orthometric height in each point) were obtained. The partial load of the engine was calculated using these data and the equations from the ASABE standards [24, 27]. With this partial load, the work regime of the engine was obtained from the curves shown in **Figure 3**. Then, the corresponding emission factor for each exhaust substance was estimated with these data and the ISO 8178 standard [26]. The ISO standard defines the emissions factors of exhaust gases for agricultural combustion engines in eight individual work regimes based on the maximum power and the manufacturing year of the engine. For small engines, as in this case, the ISO standard defines the emission factors needed to calculate CO, particulate matter and NO_X + hydrocarbons. Finally, the CO_2 emissions were calculated using the chemical equation of combustion reaction (considering the other exhaust emission gases calculated with the emission factor of the ISO standard) and the measured fuel consumption.

2.2. Agricultural tasks and implements

Three different agricultural tasks were considered, each one requiring a specific agricultural implement:

- Weed control using a thermal and a row crop cultivator implement
- Weed control using an herbicide patch sprayer
- Pest control using a canopy sprayer.

Figure 6 illustrates these three implements, and their main features and requirements are presented in the following sections. The modifications to the implements made to allow use with the hybrid energy system are also described.

2.2.1. Weed control with a thermal implement and cultivator implement

This task consisted of performing weed control using plowing and thermal treatments with a particular mechanical-thermal machine. The weed detection system detected weed patches by processing the images from a vision camera in real time. The autonomous robot was programmed to follow an initial predefined path, which fixed the initial and final points of each track (the path followed by the vehicle through the crop). However, the initial path was corrected with information provided by the row detection system based on the vision camera of the weed detection system. The area analyzed in each image was a 3-m-wide (4 rows) and 2-m-long rectangle. It was georeferenced with an accuracy of approximately 0.08 m and divided into 0.25 × 0.25 m cells [14].

The implement consisted of a row crop cultivator and thermal device. The row crop cultivator performed a mechanical treatment in the furrows (the spaces between crop rows, similar to a conventional row crop cultivator). The thermal device consisted of several burners that produced flames applied in each row for weed control. This implement (see **Figure 6a**) was used for wide rows of crops, with rows separated by approximately 0.75 m. This technique can be applied to crops that can withstand high temperatures over short periods of time, such as

Figure 6. Implements working: (a) thermal and row cultivator, (b) canopy sprayer and (c) patch sprayer.

maize, garlic, leek and onion. The implement was controlled from the main controller, which was able to regulate the gas pressure of each burner separately in three stages: zero (off), low and high. The basic features of this implement are provided in **Table 3** [28].

The implement originally had two hydraulic cylinders to allow the main bar to extend (for treatment) and retract (during transportation). These cylinders could be replaced by linear actuators with electrical motors (LINAK LA36, Guderup, Nordborg, Denmark), reducing the power demand from the internal combustion engine and increasing the power demand from the electrical energy system. The power demand from the electrical energy system was relatively small because plowing was the main energy demand of this task, and the energy required for plowing was supplied by the internal combustion engine. This implement used gas fuel for the burners, but the gas fuel was not considered in the energy analysis; the energy analysis considered only the electrical power used to light the burners. Any type of biogas could be used for the burners, which have negligible combustion emissions.

Implement	Feature	Value
Thermal and row crop cultivator	Power of the implement controller	40 W (24 V)
	Number of burners (two per row)	8
	Power of the valves and sensors	<1 W
	Power of each ignitor	144 W (24 V)
	Linear actuator engine power (×2)	240 W (24 V)
Patch sprayer	Power of the implement controller	40 W (24 V)
	Number of nozzles	12
	Nominal flow of the nozzles	0.0126 L s^{-1}
	Nominal pressure of the nozzles	2.76 10^5 Pa
	Power of each pump	16.5 W (24 V)
	Power of the flow control system	15 W (12 V)
	Engine power of each linear actuator (×2)	200 W (12 V)
Canopy sprayer	Power of the implement controller	40 W (24 V)
	Number of diffusors	8
	Nominal flow of the nozzles (two per diffusor)	0.066 L s^{-1}
	Nominal pressure of the nozzles	3 10^5 Pa
	Power of each pump	19 W (24 V)
	Power of the flow control system	24 W (24 V)
	Air flow per nozzle	~0.5 m^3 s^{-1}
	Power of each fan	105 W (24 V)
	Power of the ultrasonic sensors	12 W (24 V)
	Engine power of each angle regulator (×4)	36 W (24 V)

Table 3. Main features of the implements [12, 31–33].

2.2.2. Weed control with an herbicide patch sprayer

This task consisted of spraying herbicides over weed patches of herbaceous crops. The weed patches were detected and localized using the remote weed detection system, which was a system based on vision cameras that acquired images using aerial robots and provided a weed map of the crop consisting of 0.25 × 0.25 m cells with weed indexes indicating the percentage of each cell's area covered by weeds with respect to the total cell area. This map is an input for the autonomous robot, which will open/close the implement nozzles over the cells depending on their cell weed indexes.

The implement was a conventional patch sprayer (see **Figure 6c**) modified to activate each nozzle separately and regulate the total flow of the applied product. Two electrical linear actuators extended and retracted the spraying booms that were controlled by the robot's central controller. The main features of this implement are summarized in **Table 3** [29].

Originally, this implement used a main pump that worked with the PTO using the internal combustion engine's power. The pump worked to a rated power whenever a valve was open and used a bypass line to return the product overflow, wasting a large amount of energy. To improve this system, the main pump was replaced with a set of small pumps, using one pump for each nozzle. The selected pump for this application was the model MG100 Micropump (TCS Micropumps Ltd., Faversham, Kent, UK), which was able to regulate the flow to provide sufficient flow and pressure. The implement control system was able to regulate the main herbicide flow (the total nozzle flow) to ensure correct operation. This modification generated a significant reduction in power demand from the combustion engine and increased the power demand from the electrical energy system slightly.

2.2.3. Pest control with a canopy sprayer

This task consisted of spraying insecticide into tree canopies for pest control. The robot path plan provided the initial and final points of each track, and the robot controller was responsible for interpolating the path to follow. The implement was a canopy sprayer (see **Figure 6b**) that sprayed a pesticide solution over the tree canopies and blew the spray along the entire canopy. The canopy sprayer was designed to spray trees planted in rows spaced approximately 4 m apart, a common row spacing in olive groves. The implement was autonomous, that is, capable of detecting the tree canopies and applying pesticide doses depending of the canopy dimensions. The autonomous robot central controller turned the implement on and off only at the start and end of the mission, respectively. The sprayer had four vertically placed diffusors on each side, four of which (the lower and upper) allowed the spray direction to the canopy to range from −15 to 15° with respect to its initial vertical position. Each diffusor was equipped with two nozzles and one air outlet, and the implement control system was able to activate each diffusor separately. Eight ultrasonic sensors were used to detect the tree canopy, activate the required diffusors and regulate the diffusor positions. In addition, the sprayer regulated the main flow of pesticide and air using a main pump and fan. **Table 3** shows the main features of this implement [30].

Analogous to the patch sprayer, the canopy sprayer originally used the internal combustion engine power from the PTO to operate the main pump and the fan that diffuses the pesticide throughout the tree canopy. Because this implement was autonomous, the robot's central

controller could not determine the instantaneous power requirements of the task. Thus, the pump and fan worked continuously at the rated power, wasting large amounts of energy. The system could be improved using a similar process as the previous application: replacing the main pump with a series of small pumps, replacing the main fan with a set of small fans and using one pump and one fan in each diffusor. The pump model MG100 Micro Pump and the axial compact fan EC W1G250-HH37-52 (ebm-papst Group, Mulfingen, Baden-Württemberg, Germany) were used for this modification. In this implement, the pesticide flow was controlled while the fan was maintained at its rated power. The reduction in power demand from the internal combustion engine was the largest of the three tasks, as it was the total power consumed by electrical devices.

3. Path planning to reduce the fuel consumption

To find a path plan that minimizes the fuel consumption, a number of different possible paths must be simulated. These paths must consider all possible track angles, field's slopes and vehicle mass losses during the spraying task. **Figure 7** shows the block diagram of the procedure. The first step is to obtain (a) the field and crop data, (b) the digital elevation model and (c) the weed map, and to define potential angles for the first track of the path plans to accomplish the treatment. The procedure relies in calculating the required energy of each path, considering that we can start the treatment from both sides of the crop (right or left) and rejecting the track with no weed. Finally, the plan with the smallest fuel consumption is selected.

Fuel consumption for all possible track angels, from 0 to 360°, must be calculated because for treatments with mass losses, the motion resistance at a given point may differ. Thus, the instantaneous motion resistance at each point depends on the path plan starting point [25].

The crop limits were defined as a function of the crop features and the weed map, if available, was provided by an external device. The weed maps were represented in gray scale images using eight bits per color channel; they have a pixel size of 0.5 m and were georeferenced by the position of the lower left pixel with geodesic coordinates that are translated to the (Universal transverse Mercator) UTM. The WGS84 standard Earth reference ellipsoid was used. To estimate the terrain elevation model, the GeoTIFF ASTER GDEM images obtained from the NASA website were used. These data were provided using a 1-arc-second (approximately 30 m at the Equator) grid and are referenced to the WGS84 [34].
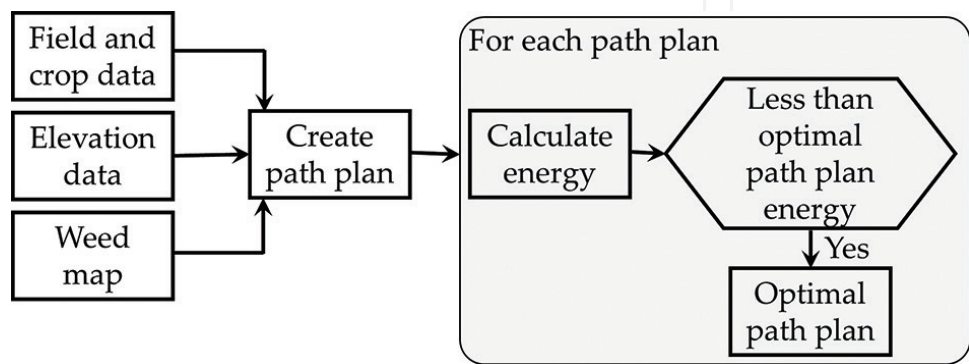
Figure 7. Path plan selection.

Implement	Implement method	Fuel consumption calculated	Fuel consumption measured
Thermal and row cultivator	Without optimization	0.48 L	0.50 L
	With optimization	0.31 L	0.43 L
	Reduction	36%	13%
Patch sprayer	Without optimization	0.74 L	0.90 L
	With optimization	0.29 L	0.53 L
	Reduction	61%	41%
Canopy sprayer	Without optimization	0.37 L	0.45 L
	With optimization	0.35 L	0.43 L
	Reduction	6%	5%

Table 4. Results in fuel optimization.

Table 4 summarizes the results obtained with these methods, and **Figure 8** represents the best path plan to reduce the fuel consumption.

For the path sprayer case, where the areas to be treated are known in advance, the fuel reduction resulted the best. Thus, a weed detection system that provides the weed data in advance, with the consequent energy cost, is essential. However, this study considers that energy negligible with respect to the energy savings achieved. In the case of the thermal and row cultivator implement, we know the areas to be treated a few seconds before the treatment, but it suffices for applying some energy-saving actions to obtain an important energy reduction.

Finally, in the case of the canopy sprayer, an autonomous implement capable of detecting the areas to be treated a few milliseconds in advance is used. This implement does not enable the use of nearly any energy-saving actions, and the fuel reduction obtained is thus the lowest.
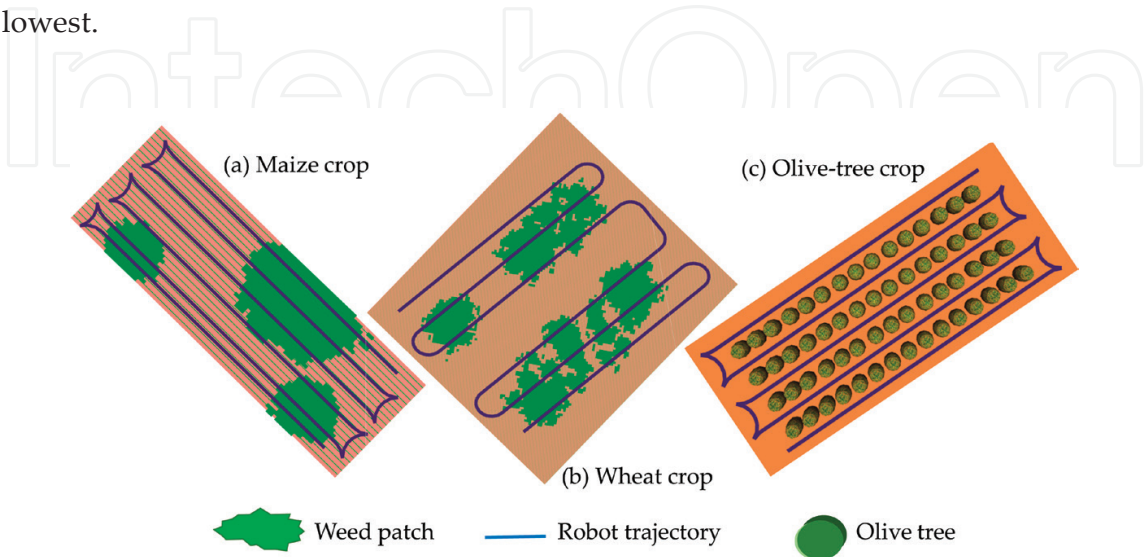

Figure 8. Test field schemes with the best path planning.

4. Energy demand analysis

To estimate the total energy consumed in each agriculture task, the instantaneous power, the time and the relationship with the energy source were all related. The robot had four energy sources: fuel, hydrogen, batteries and solar power (the instantaneous power provided by the Sun cannot be regulated). The energy demand has two main components:

- The energy demand supplied by the internal combustion engine, E_{ICE}, which is the energy used to move the robot and implement.

- The electrical energy demand supplied by the electrical energy system, E_{EES}.

- Thus, the total energy consumed, E_T, could be calculated as follows [35]:

$$E_T = E_{ICE} + E_{EES} \tag{4}$$

The energy provided by the internal combustion engine, E_{ICE}, can be computed as

$$E_{ICE} = \int_0^T P_{ICE}(t)\, dt = \int_0^T \left(D(t) + F_{MR}(t)\right)v(t)dt \tag{5}$$

where v is the system speed; D is the implement draft force, which depends on the dimensionless soil texture adjustment parameter and machine-specific parameters; F_{MR} is the motion resistance force, which depends of the soil surfaces, terrain slope, wheel slippage, total system mass and vehicle tires; and T is the study period. Eq. (5) computes the energy obtained from an internal combustion engine, but it does not consider the loss of mechanical and traction efficiencies in the vehicle [24, 27].

The second term of Eq. (4), that is, the energy supplied by the electrical energy system, can be calculated by

$$E_{EES} = \int_0^T P_{EES}(t)\, dt = \int_0^T \left(P_{AR\_control}(t) + P_{IMP\_control}(t) + n\, P_{Tool}(t)\right) dt \tag{6}$$

where P_{EES} is the instantaneous power demanded to the electrical energy system, $P_{AR\_control}$ is the power used to supply the autonomous robot controller described in Section 2.1.1, $P_{IMP\_control}$ is the power consumed by the electrical system of the implement (e.g., controllers, sensors and position actuator), n is the number of active tools and P_{Tool} is the electrical power consumed by each tool. A tool is defined as a set of systems that can be activated separately to apply the treatment correctly in a given zone. With the thermal and row cultivator implement, the tool was the set of two burners and hoes used in each crop row, which used two ignitors (only to light the burners) and two valves (only to change the tool status). In the patch sprayer, the tool was each nozzle, each of which used a pump. In the canopy sprayer, the tool was the set of two nozzles and the air outlet of each diffuser, each of which used a pump and fan. Eqs. (4)–(6) describe the model of the energy demand in the system for a specific task.

5. Energetic analysis

This section studies the energy requirements of the aforementioned agricultural tasks and the required features and devices of the hybrid energy system.

5.1. Energy demanded in the selected task

The energy required for the autonomous robot and implement in each of the aforementioned agricultural tasks was estimated using a representation of real crops (see **Figure 8**). The energy analysis described in Section 4 was used to estimate the total energy consumed, measured as both the maximum power demand and average power. The power was split into two values: (1) the power demanded by the 24-V DC system and (2) the power demanded by the 12-V DC system.

5.1.1. Energy analysis of weed control using a thermal implement and cultivator implement

The electrical power demands of the 12-V DC devices, 24-V DC devices and their combined sum are shown in **Figure 9a**. In this application, the power demand from the 12-V DC devices was approximately constant, and the power demand of the 24-V DC system had abrupt and short peaks, which were generated by the ignition of the burners. **Table 5** presents the values of these peaks and the average values of each type of power demand.

The total hydrogen consumed during a working shift of 8 h was calculated under the assumption that the hydrogen fuel cell, which was described in Section 2.1.3, supplied all of the electrical energy. This task represented the lowest power demand from the electrical energy system because the energy for plowing was supplied by the internal combustion engine and the gas burners did not require electrical power to work, only an ignition spark. Thus, the electrical energy system was mainly used to power the electrical control systems.

5.1.2. Energy analysis of weed control using a patch sprayer

Figure 9b illustrates the instantaneous power demand of the patch sprayer in a weed control task. The power consumed by the 12-V DC system was approximately constant because this power was mainly used to supply energy to the system controllers. However, the power demanded by the 24-V DC system, used to provide power to the implement devices, exhibited important variation that occurred when the pumps applied the treatment to weed patches. The maximum values of the power demand, their average values and the total hydrogen consumed during an 8-h work shift are shown in **Table 5**. These values were generally higher than those for the above case.

5.1.3. Energy analysis of pest control tasks using a canopy sprayer

As in previous tasks, **Figure 9c** shows the power required for pest control using the autonomous canopy sprayer. These graphs are similar to the patch sprayer application but with larger values for the power demanded by the 24-V system, the only voltage used in this implement. The numerical values (and comparisons) for power demand in the pest control task, and other tasks are provided in **Table 5**. As expected, the pest control task had the highest
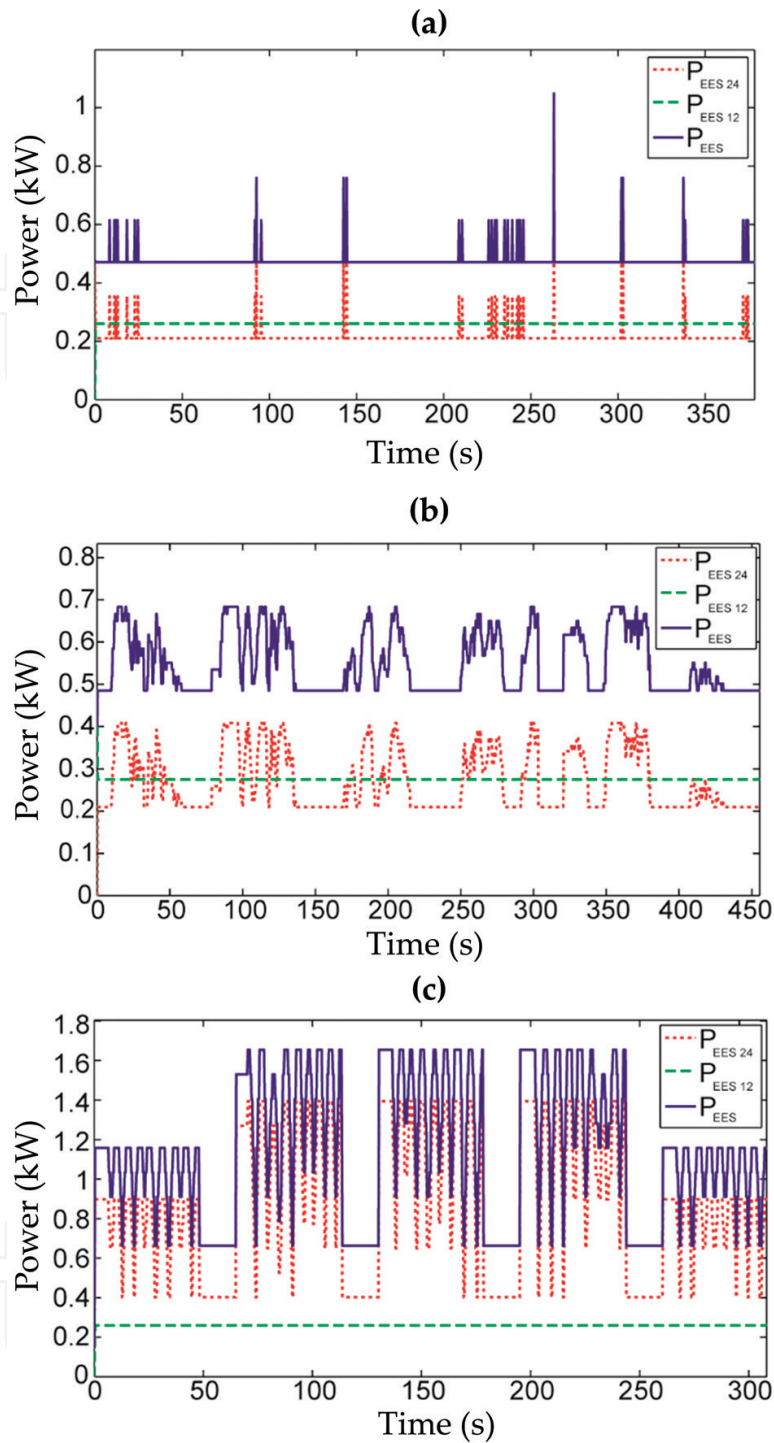
Figure 9. Power demands of the electrical energy system (ESS): (a) weed control using the thermal and row crop cultivator implement; (b) weed control using the sprayer implement and (c) pest control using the canopy sprayer. $P_{EES\,12}$, $P_{EES\,24}$ and $P_{ES}S$ are the 12-V, 24-V and total power, respectively.

power demand from the electrical energy system, although the power demand from the 12-V DC system was similar to the other three cases because it was used mainly to supply the controllers. Thus, the controllers had a quasi-constant power demand and were not strongly influenced by the task.

	Implement		
	Thermal and row crop cultivator	Patch sprayer	Canopy sprayer
12-V average power	0.26 kW	0.28 kW	0.26 kW
24-V average power	0.22 kW	0.28 kW	0.90 kW
Total average power	0.48 kW	0.56 kW	1.16 kW
12-V maximum power	0.26 kW	0.40 kW	0.26 kW
24-V maximum power	0.79 kW	0.41 kW	1.39 kW
Total maximum power	1.05 kW	0.68 kW	1.65 kW
H_2 consumed (for 8 h)	2.43 Nm^3	2.84 Nm^3	5.96 Nm^3

Table 5. Power and hydrogen consumed in each application.

5.2. Hybrid energy system

The energy system studied in this work used the original internal combustion engine of the tractor operating in parallel with an electrical energy system. The architecture of the resulting hybrid energy system is shown in **Figure 10**. The internal combustion engine was used to provide motion, overcoming the motion resistant force and possible draft forces generated by the implement, while the electrical energy system was used to power all electrical systems onboard the autonomous robot. The combustion engine had enough power and autonomy for the tasks analyzed in this work, but an electrical energy system was needed to supply the electrical energy required for each agricultural task.

The electrical energy system used hydrogen as the main energy source, with a small contribution from a photovoltaic panel, and used batteries to adapt the power supply to the energy requirements and store excess electrical energy generated by the photovoltaic panel when it was not in use. The electrical energy system was designed according to the maximum values in **Table 5**.

The hydrogen system was designed to supply the average power demanded by all electrical systems, for example, control systems, sensors and actuators. Therefore, a hybrid fuel cell with a minimum power of 1.16 kW and at least 5.96 Nm^3 of hydrogen storage was required.

The hybrid fuel cell was based on the TROPICAL TB-1000 model. It was an unregulated DC power system based on a proton exchange membrane fuel cell (FCgen-1020ACS, Ballard Power Systems, Burnaby, British Columbia, Canada). The system had to be fueled with pure hydrogen and was able to deliver up to 1.4 kW of peak electrical power and 1.2 kW in a nominal continuous operation. A hydrogen storage system based on metal hydride tanks was used. Four tanks were used, each with a capacity of 3 Nm^3.

The photovoltaic panel was a Module EGM-185 (EGing PV Co., Ltd., Jintan, Jiangsu, P.R. C), which had a power rating of 183 W and an efficiency of approximately 15%. At the test site location (40°18′29″ N, 3°29′14″ W), this panel provided an average daily energy amount of
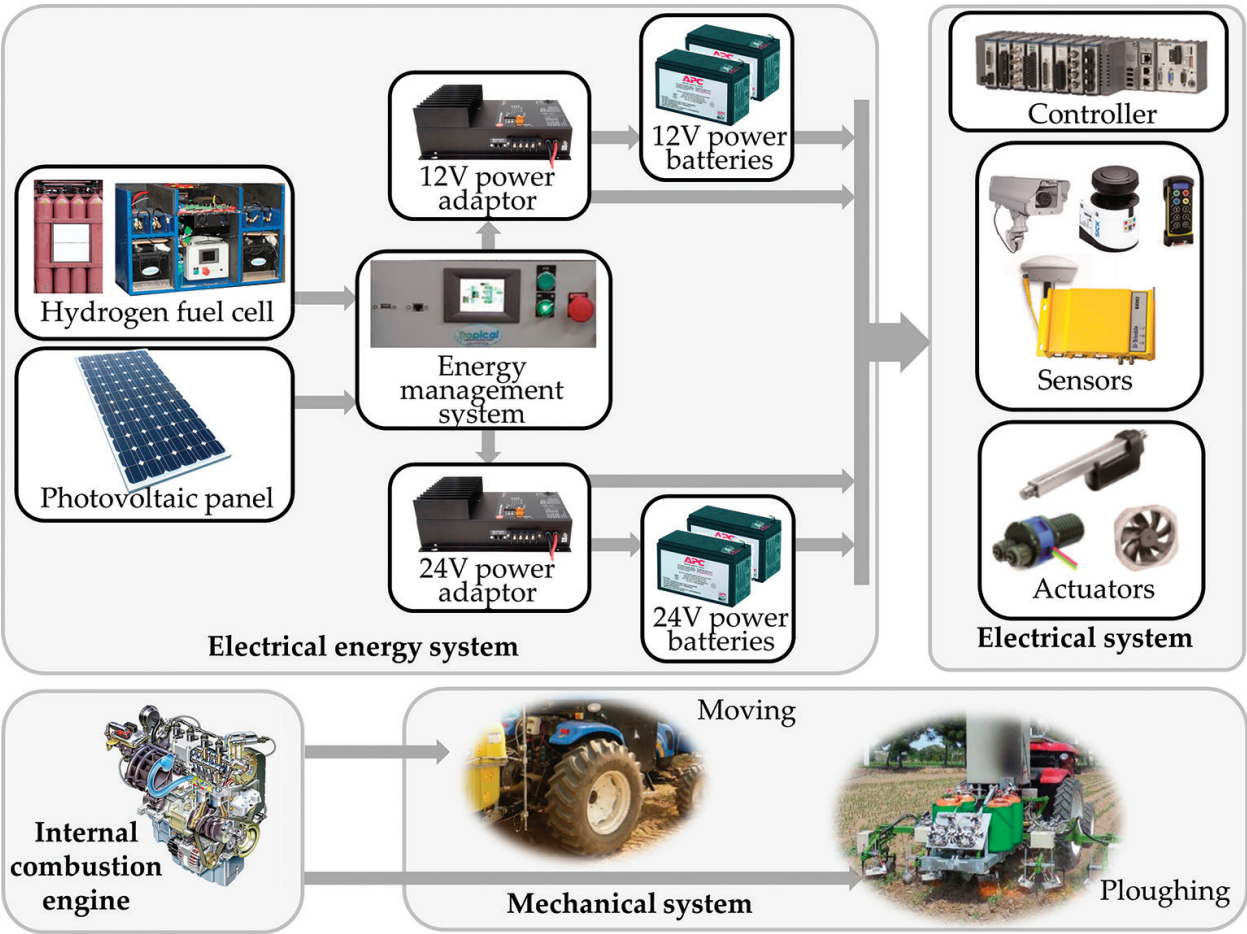
Figure 10. Hybrid energy system.

0.88 kWh, with a maximum of 1.46 kWh per day in July, according to the irradiation data available from the Photovoltaic Geographical Information System of the Institute for Energy and Transport [36].

Deep-cycle lead-acid batteries, which could supply current levels greater than those provided by the hybrid fuel cell over short periods, were used. The lead-acid batteries were charged by both the hybrid fuel cell and photovoltaic panel and stored all unused photovoltaic energy. The batteries were divided into two banks to supply 12 V DC and 24 V DC. Each bank consisted of two batteries, each with a capacity of 2.2 kWh; this capacity was sufficient to store excess photovoltaic energy over several days of inactivity and could be used during sporadic periods of high energy demand, as shown in **Figure 11**. **Table 5** shows that the power demand of the 24-V DC system was higher, but this analysis did not consider the energy required to start the combustion engine. Furthermore, two or more batteries in parallel were required to start the internal combustion engine because deep-cycle batteries were used.

The energy management system was responsible for

- Regulating and adapting the power provided by the hydrogen fuel cell and photovoltaic panel.

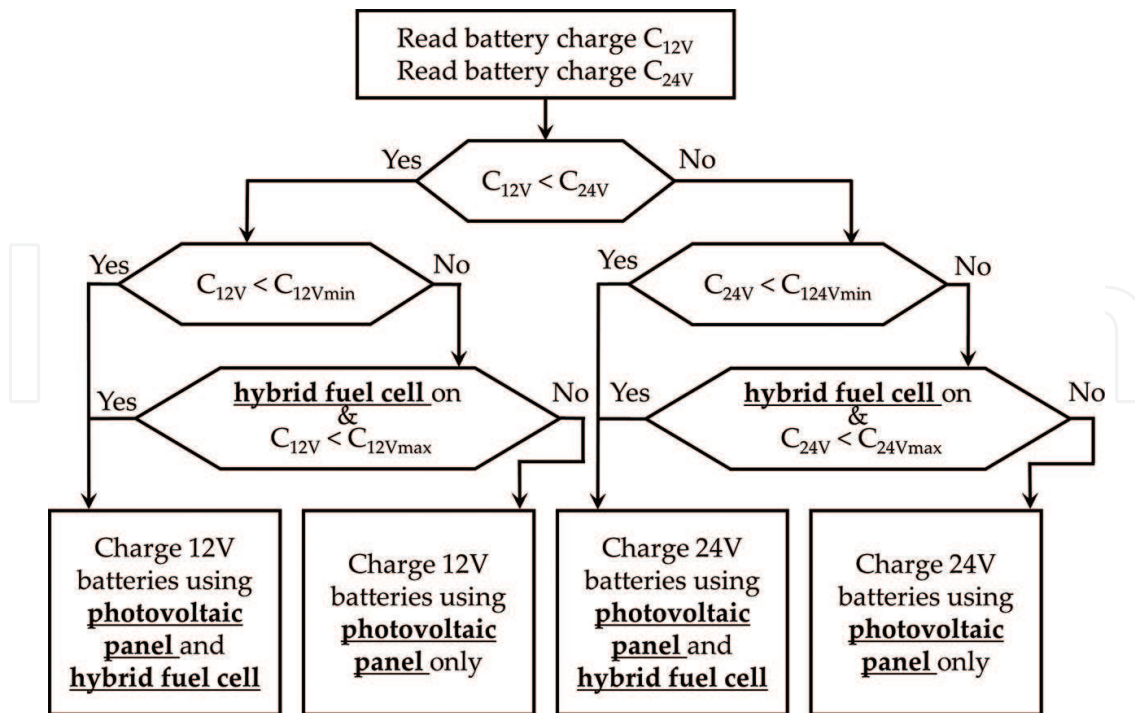- Assuring a minimum charge in the batteries.

Figure 11. Block diagram of the flow energy control.

- Obtaining the maximum photovoltaic power.

- Supervising the hydrogen storage, batteries status and photovoltaic power.

The energy management system used two solar-panel controllers (either 12-V batteries or 24-V batteries) with the maximum power point tracking (MPPT SS-MPPT-15 L, Morningstar, Inc., Chicago, Illinois, US) to obtain the maximum power from the photovoltaic panel.

Both 12-V and 24-V battery chargers (or power adapters) (BCD1015, Analytic Systems Ware Ltd., Delta, British Columbia, Canada) were required to adapt the power from the hybrid fuel cell. The energy management system was equipped with a controller that managed the energy flow. The block diagram of the energy management system is shown in **Figure 11**, where C_{12V} and C_{24V} are the charges of the 12-V and 24-V batteries, respectively; C_{12Vmin} and C_{24Vmin} are the minimum charges in these batteries with the hybrid fuel cell stopped; and C_{12Vmax} and C_{24Vmax} are the maximum charges in these batteries when the hybrid fuel cell is running. C_{12Vmin} and C_{24Vmin} were calculated to ensure correct operation during periods of high energy demand. The C_{12Vmax} and C_{24Vmax} values were calculated to create a hysteresis cycle for the hybrid fuel cell's operation with a value that is sufficiently high to avoid excessive start/stop in the hybrid fuel cell but sufficiently low to allow for the storage of the photovoltaic energy generated when the robot was stationary.

6. Results and discussion

This section presents the emission reductions obtained by using the hybrid energy system in real scenarios. To analyze the results, the emissions of the autonomous robot with the

internal combustion engine as the only power system were compared with the emissions of the same robot using the additional hybrid energy system described in Section 5.2. The same autonomous mobile robot was used in all tests, and the fuel consumption and emissions were measured as explained in Section 2.1.7. The experiments were carried out for the crops and tasks introduced in Section 2.2, and the results are described in the following sections.

6.1. Hybrid power of weed control with a thermal implement and a cultivator implement

This test was performed over the maize crop represented in **Figure 8a**, where the path followed by the robot is indicated in blue and the weed patches are indicated in green. As described in Section 2.2.1, the vision system onboard the robot detected the weed patches in real time; therefore, the trajectories had to cover the entire field because a priori knowledge of where the patches were located was not available. Although the burners were activated only over weed patches, the hoes plowed all furrows to kill weeds and aerate the soil. Therefore, the energy required to plow all tracks was high, and more exhaust gas was produced, particularly CO_2, as shown in **Figure 12a**, which shows the exhaust gas emitted as a function of the distance traveled. The required energy to plow was the main power demand supplied by the engine in both cases (using the internal combustion engine alone and using it along with the hybrid energy system). Consequently, the emission reduction obtained due to the use of the hybrid energy system was small.

As shown in **Figures 12a–d** and **Table 6**, the reduction in air pollution during this task was lower than in the other analyzed tasks. The CO_2 emissions were only slightly reduced as a result of the energy consumed by the burner ignitors and electrical control system, although the energy consumed by the ignitors was relatively negligible.
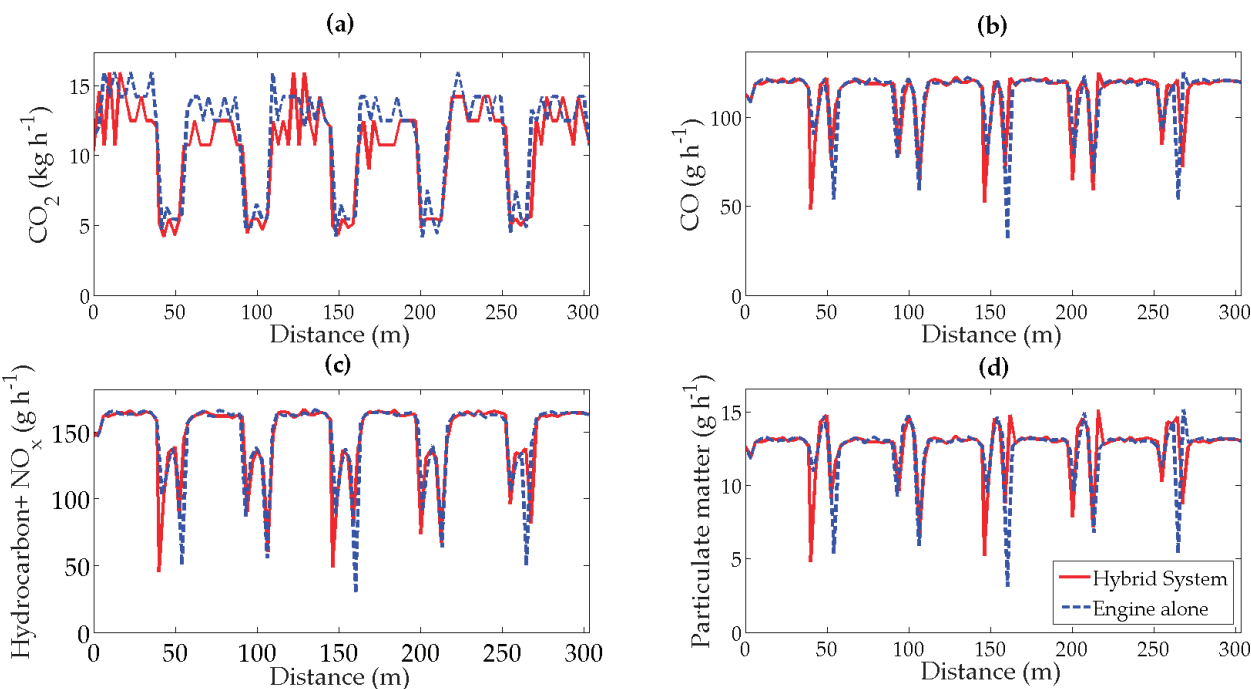
Figure 12. Exhaust gas emissions in weed control using the thermal and row crop cultivator implement.

Application	Power system	CO_2	CO	$HC + NO_x$	PM
		(kg h^{-1})			
Thermal and cultivator	Combustion engine only	11.32	0.1132	0.1478	0.0126
	Hybrid system	10.36	0.1129	0.1475	0.0126
	Exhaust gas reduction	8.53%	0.2%	0.2%	0.0%
Patch sprayer	Combustion engine only	9.86	0.1334	0.1852	0.013
	Hybrid system	6.25	0.110	0.1434	0.0123
	Exhaust gas reduction	36.6%	17.8%	22.6%	5.4%
Canopy sprayer	Combustion engine only	10.74	0.1425	0.2047	0.0125
	Hybrid system	5.64	0.1071	0.1393	0.012
	Exhaust gas reduction	47.5%	24.8%	31.9%	3.8%

Table 6. Average values and comparison of exhaust gas emissions in the three applications.

6.2. Hybrid power of weed control with an herbicide patch sprayer

This test was performed over the wheat crop represented in **Figure 8b**, where the path followed by the robot is indicated in blue and the weed patches are indicated in green. The weed map was acquired in advance using remote sensing. Thus, the robot did not need to move over the entire field, as in the task described in Section 2.2.2, and the path could be optimized to pass over only the weed patches, reducing energy consumption.

Figure 13 shows the instantaneous emissions of CO_2, CO, hydrocarbons + NO_x and particulate matter obtained in this experiment, and **Table 6** shows their average values and the
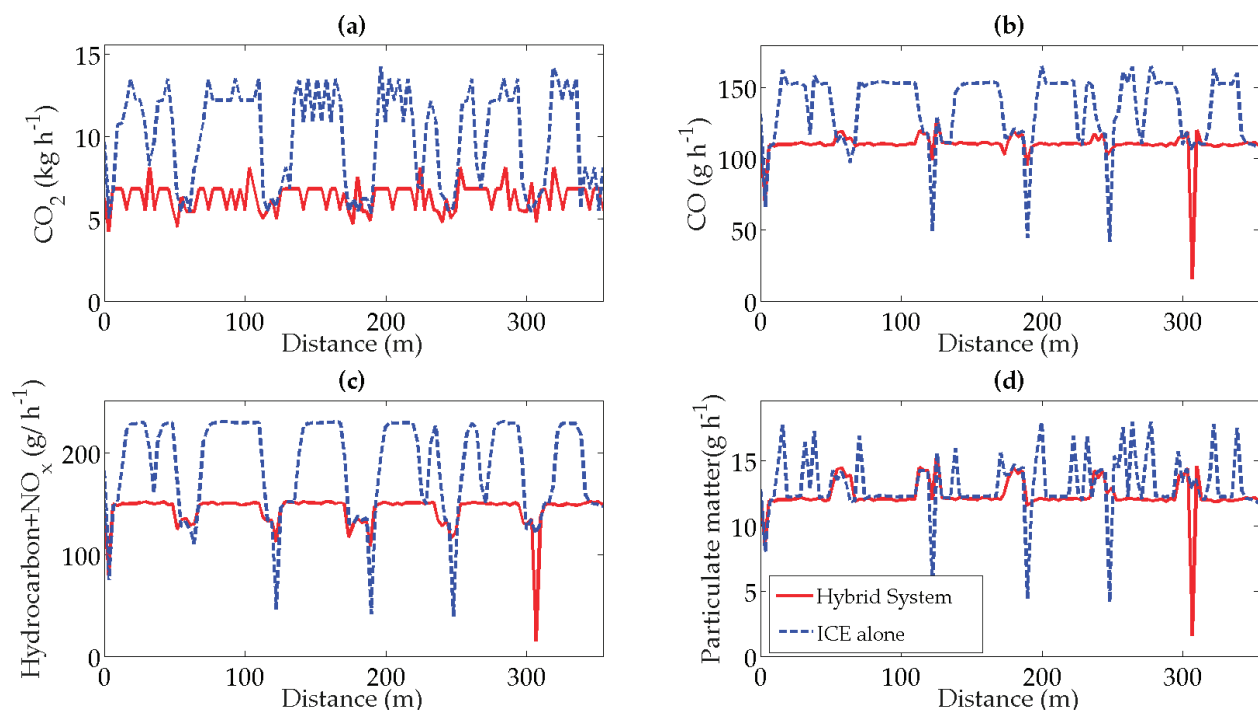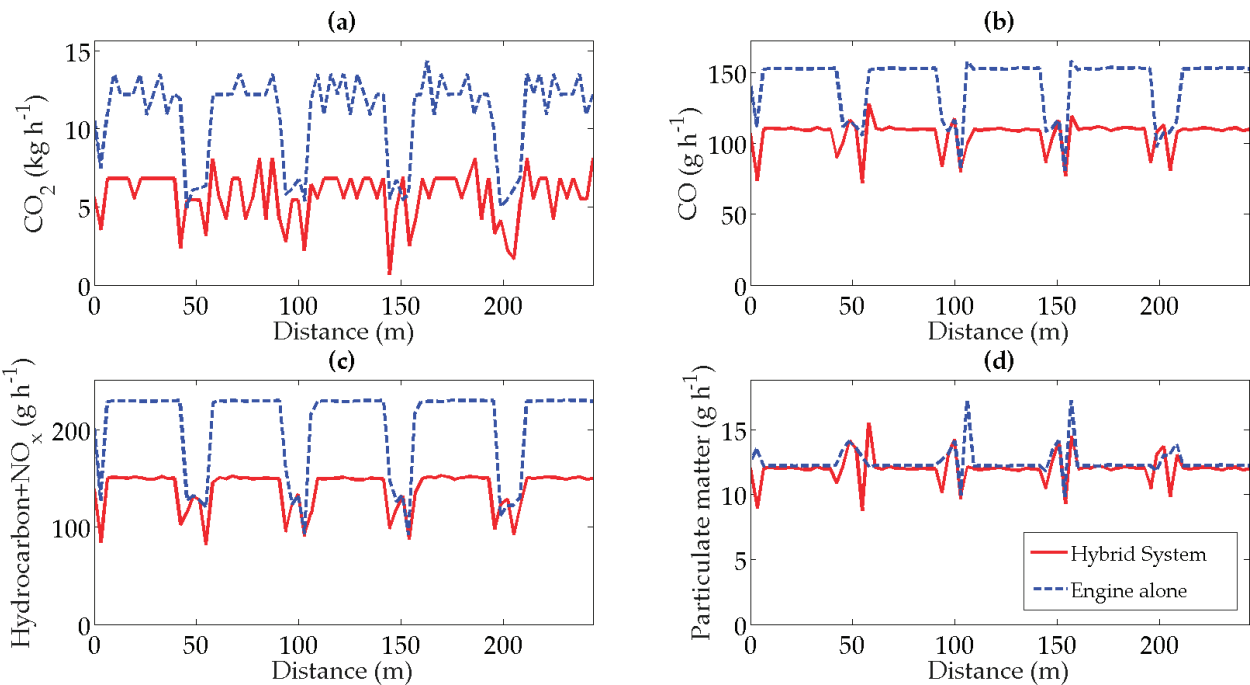

Figure 13. Exhaust gas emissions in weed control using the patch sprayer.

reductions obtained when using the hybrid energy system. **Figure 13a** shows a significant reduction in CO_2 emissions because the hybrid energy system avoids the use of the PTO, resulting in a significant reduction in fuel consumption.

Figure 13c presents the reductions in hydrocarbon and NO_x emissions, but these reductions were smaller than the reduction in CO_2 because the NO_x concentration in the exhaust gases decreased with engine speed but the concentration of hydrocarbons increased. Particulate matter emissions were highly similar in both cases (see **Figure 13d**) because their concentrations in the exhaust gases increased as the engine speed decreased, which occurred when the PTO was off or operating slowly. A similar result, but to a lesser extent, was obtained for CO, as shown in **Figure 13b** and **Table 6**.

6.3. Hybrid power of pest control with a canopy sprayer

This test was performed in the small olive grove represented in **Figure 8c**, where the path followed by the autonomous robot is indicated in blue and the olive trees are indicated in green. The implement used for this task was the autonomous canopy sprayer, as described in Section 2.2.3. This implement, as discussed in Section 5.1.3, demanded the majority of the energy from the electrical energy system out of the three experiments that were conducted. The highest reduction in power demand from the combustion engine was achieved in this experiment, resulting in the highest reduction in the exhaust gases, as illustrated in **Figures 14a–d** and **Table 6**. The reduction in CO_2 emissions reached approximately 50%. The results are similar to the previous experiments (herbicide spraying) but, in general, with a greater reduction in emissions.

Figure 14. Exhaust gas emissions in weed control using the patch sprayer.

7. Conclusions

This work demonstrates that using fuel optimization techniques with a good consumption model combined with field data (field limits and field elevation map) and crop needs can achieve fuel savings of approximately 50% in the best case. Furthermore, it is proved that to combine current agricultural machines, which use combustion engines for power, with new technologies that are based on clean energy sources to significantly reduce the emissions of atmospheric pollutants and greenhouse gases. This integration can be accomplished by offloading the combustion engine and adding this load to an additional electrical energy system. This technique was highly effective for tasks where the implement requires PTO power, as shown in Sections 6.2 and 6.3. The replacement of this PTO power is relatively simple; only small modifications were required in the implement, as described in Section 2.2. When the implement generated draft force (e.g., in plowing), this technique was not as effective as in the experiments analyzed in Sections 6.2 and 6.3; however, a reduction in the pollutant emissions was obtained from the robotic systems when electrical energy consumption was important.

The use of electrical energy systems allows small electrical actuators to be used, which are able to apply treatments to small areas with little power consumption. The use of such distributed systems is particularly important in precision agriculture, where treatments must be focused only on affected areas, which are often smaller than the total area that the implement is able to treat.

The greatest improvement was obtained by the autonomous implement analyzed in Section 6.3. In this example, the robot does not know the instantaneous power requirements of the implement, and thus, for the case in which the combustion engine is the only power source, the engine must supply the rated power to the implement, which is an inefficient use of energy. However, with the hybrid energy system, the implement uses the energy provided by the electrical energy system, and it is able to manage and minimize its energy.

The CO and particulate matter emissions present the least reduction because these concentrations of emissions were larger when the hybrid energy system was used due to the effect of decreasing engine speed. Similar emission results were obtained for these gases in many studies that analyzed internal combustion engine exhaust gases [5, 6, 37]. But, although the concentrations of CO and particulate matter in the exhaust gases were lesser for these engine speeds and loads, the total exhaust gases increased because the flow of exhaust gases emitted from the combustion engine was much greater than the gases from the hybrid energy system. The theoretical studies and experiments conducted in this work reveal that the use of a hybrid energy system in precision agriculture via autonomous robots improves the quality of the exhaust gases and decreases energy use. Compared with traditional tractors, robotic tractors have increased electric power consumption; therefore, an electrical energy system must be added when the agricultural vehicle is robotized because the use of alternators increases energy loss. Furthermore, an electrical energy system can be designed to supply some of the energy requirements of various agricultural tasks, as shown in this work. The hybrid energy system significantly reduced atmospheric pollutant emissions, including CO_2, CO, NO_x, hydrocarbons and particulate matter. This work has demonstrated that hybrid energy

systems can be reliably and autonomously used in agricultural tasks with tractors or robots, decreasing (to various extents) the load on the internal combustion engine. This development can be regarded as an intermediate step toward the use of completely clean energy systems.

Acknowledgements

Nomenclature

Chemical components

CO   carbon monoxide

CO_2 carbon dioxide

NO_X nitrogen oxides

SO_2 sulfur dioxide

Symbols

D implement draft force (N)

E_{ICE} energy demand supplied by the internal combustion engine (Wh)

F_{MR} total implement motion resistance (N)

n number of tools

P_{Tool} electrical power of each implement tool (W)

V_{TFC} total fuel consumed (L)

V_{SFC} specific fuel consumption volume (L Wh^{-1})

E_T total energy (Wh)

P_{PTO} power requirement from the PTO shaft (W)

P_{PTOeq} equivalent PTO power (W)

$P_{PTOrated}$ rated PTO power (W)

P_{T_PTOeq} total equivalent PTO demanded power (W)

$P_{AR\_control}$ power used to supply the autonomous robot controller (W)

$P_{IMP\_control}$ power consumed by the electrical system of the implement (W)

n_{PT} partial throttle engine speed (rpm)

n_{FT} full throttle engine speed (rpm)

P_{hyd} hydraulic power (W)

P_{el} electrical power (W)

Acronyms

DC   direct current

NASA   The National Aeronautics and Space Administration

PTO   power take-off

GPS   global positioning system

RTK   real-time kinematic

UTM   Universal transverse Mercator

WGS84   World geodetic system of 1984

Author details

Mariano Gonzalez-de-Soto, Luis Emmi and Pablo Gonzalez-de-Santos*

*Address all correspondence to: pablo.gonzalez@csic.es

Centre for Automation and Robotics (UPM-CSIC), Madrid, Spain

References

[1] U.S. Environmental Protection Agency (EPA). http://www.epa.gov/ [Accessed: January 4, 2018]

[2] Hansson PA, Lindgren M, Noren O. PM-power and machinery: A comparison between different methods of calculating average engine emissions for agricultural tractors. Journal of Agricultural Engineering Research. 2001;**80**:37-43. DOI: 10.1006/jaer. 2001.0710

[3] Dalgaard T, Halberg N, Porter JR. A model for fossil energy use in Danish agriculture used to compare organic and conventional farming. Agriculture Ecosystems & Environment. 2001;**87**:51-65. DOI: 10.1016/S0167-8809(00)00297-8

[4] Peltre C, Nyord T, Bruun S, Jensen LS, Magid J. Repeated soil application of organic waste amendments reduces draught force and fuel consumption for soil tillage. Agriculture Ecosystems & Environment. 2015;**211**:94-101. DOI: 10.1016/j.agee.2015.06.004

[5] Lindgren M, Arrhenius K, Larsson G, Bäfver L, Arvidsson H, Wetterberg C, et al. Analysis of unregulated emissions from an off-road diesel engine during realistic work operations. Atmospheric Environment. 2011;**45**:5394-5398. DOI: 10.1016/j.atmosenv.2011.06.046

[6]   Janulevičius A, Juostas A, Pupinis G. Tractor's engine performance and emission characteristics in the process of ploughing. Energy Conversion and Management. 2013;**75**:498-508. DOI: 10.1016/j.enconman.2013.06.052

[7]   Gasparatos A, Stromberg P, Takeuchi K. Biofuels, ecosystem services and human well-being: Putting biofuels in the ecosystem services narrative. Agriculture Ecosystems & Environment. 2011;**142**:111-128. DOI: 10.1016/j.agee.2011.04.020

[8]   Mousazadeh H, Keyhani A, Javadi A, Mobli H, Abrinia K, Sharifi A. Life-cycle assessment of a solar assist plug-in hybrid electric tractor (SAPHT) in comparison with a conventional tractor. Energy Conversion and Management. 2011;**52**:1700-1710. DOI: 10.1016/j.enconman.2010.10.033

[9]   Mulloney JA Jr. Mitigation of carbon dioxide releases from power production via "sustainable agri-power": The synergistic combination of controlled environmental agriculture (large commercial greenhouses) and disbursed fuel cell power plants. Energy conversion and management. In: Proceedings of the International Energy Agency Carbon Dioxide Disposal Symposium. Vol. 34. 1993. pp. 913-920. DOI: 10.1016/0196-8904(93)90036-A

[10] Lutz AE, Larson RS, Keller JO. Thermodynamic comparison of fuel cells to the Carnot cycle. International Journal of Hydrogen Energy. 2002;**27**:1103-1111. DOI: 10.1016/S0360-3199(02)00016-2

[11] Offer GJ, Howey D, Contestabile M, Clague R, Brandon NP. Comparative analysis of battery electric, hydrogen fuel cell and hybrid vehicles in a future sustainable road transport system. Energy Policy. 2010;**38**:24-29. DOI: 10.1016/j.enpol.2009.08.040

[12] Gonzalez-de-Santos P, Ribeiro A, Fernandez-Quintanilla C, Lopez-Granados F, Brandstoetter M, Tomic S, Pedrazzi S, Peruzzi A, Pajares G, Kaplanis G, Perez-Ruiz M, Valero C, del Cerro J, Vieri M, Rabatel G, Debilde B. Fleets of robots for environmentally-safe pest control in agriculture. Precision Agriculture. 2017;**18**(4):574-614

[13] Emmi L, Gonzalez-de-Soto M, Pajares G, Gonzalez-de-Santos P. New trends in robotics for agriculture: Integration and assessment of a real fleet of robots. The Scientific World Journal. 2014;**2014**:1-21. Article ID 404059. DOI: 10.1155/2014/404059

[14] Emmi L, Gonzalez-de-Soto M, Pajares G, Gonzalez-de-Santos P. Integrating sensory/actuation systems in agricultural vehicles. Sensors. 2014;**14**:4014-4049. DOI: 10.3390/s140304014

[15] Conesa-Muñoz J, Gonzalez-de-Soto M, Gonzalez-de-Santos P, Ribeiro A. Distributed multi-level supervision to effectively monitor the operations of a fleet of autonomous vehicles in agricultural tasks. Sensors. 2015;**15**:5402-5428. DOI: 10.3390/s150305402

[16] CNH America LLC. BOOMER 3040, 3045, 3050 CVT service manual complete contents; 2009

[17] Tropical, Fuel Cell Power Gener. Hydrog. Technol. Electr. Automob. e Trop. SA Fuel Cell Hydrog. Technol. 2018. http://www.tropical.gr/index.php [Accessed: January 4, 2018]

[18] Spanish Royal Order 61/2006 of January 31, which determines the requirements of gasoline, gasoline, fuels and liquefied petroleum gases and regulates the use of certain biofuels. Official State Gazette, February 17, 2006, no. 41. pp. 6342-6357. In Spanish

[19] International Energy Agency. Oil information: Documentation for beyond 2020 file; 2013

[20] Titan Enterprises Ltd. Titan flow meters for oil, boiler and diesel fuel applications—PD400 oil flowmeter. 2018. http://www.flowmeters.co.uk/pd_pd400om [Accessed: January 4, 2018]

[21] Grisso R, Kocher M, Vaughan D. Predicting tractor fuel consumption. Biological Systems Engineering: Papers and Publications. University of Nebraska. 2004. https://pdfs.semanticscholar.org/79db/cec98eaa6ef92be5d1c590a5dd587121b1db.pdf [Accessed: January 4, 2018]

[22] Rahimi-Ajdadi F, Abbaspour-Gilandeh Y. Artificial neural network and stepwise multiple range regression methods for prediction of tractor fuel consumption. Measurement. 2011;**44**:2104-2111. DOI: 10.1016/j.measurement.2011.08.006

[23] Titan Enterprises Ltd-Titan flow meters for oil, boiler and diesel fuel applications—PD400 oil flowmeter. 2014. http://www.flowmeters.co.uk/ [Accessed: February 20, 2014]

[24] ASAE. D497.7 MAR2011 Agricultural Machinery Management Data. St. Joseph, MI, USA: ASAE Standards; 2011. pp. 372-380

[25] Gonzalez-de-Soto M, Emmi L, Garcia I, Gonzalez-de-Santos P. Reducing fuel consumption in weed and pest control using robotic tractors. Computers and Electronics in Agriculture. 2015;**114**:96-113. DOI: 10.1016/j.compag.2015.04.003

[26] ISO 8178-4: 1996-Reciprocating internal combustion engines-exhaust emission measurement-Part 4: Test cycles for different engine applications. International Organisation of Standardisation; 1996

[27] ANSI/ASAE. S296.4 DEC95 Agricultural Machinery Management Data. St. Joseph, MI, USA: ASAE Standards; 1995. pp. 118-120

[28] Frasconi C, Martelloni L, Fontanelli M, Raffaelli M, Emmi L, Pirchio M, Peruzzi A. Design and full realization of physical weed control (PWC) automatic machine within the RHEA project. In: Second International Conference on Robotics and Associated High-Technologies and Equipment for Agriculture and Forestry (RHEA-2014); May 21-23, Madrid, Spain. 2014. pp. 3-11

[29] Perez-Ruiz M, Gonzalez-de-Santos P, Ribeiro A, Fernandez-Quintanilla C, Peruzzi A, Vieri M, Tomic S, Agüera J. Highlights and preliminary results for autonomous crop protection. Computers and Electronics in Agriculture. 2015;**110**:150-161. DOI: 10.1016/j.compag.2014.11.010

[30] Sarri D, Lisci R, Rimediotti M, Vieri M. RHEA airblast sprayer: Calibration indexes of the air-jet vector related to canopy and foliage characteristics. In: Second International Conference

on Robotics and Associated High-Technologies and Equipment for Agriculture and Forestry; May 21-23; Madrid, Spain. 2014. pp. 73-81

[31] Tecnológica Actuadores Lineales LINAK Actuadores SLuSpain Port. 2018. http://www.linak.es/ [Accessed: January 4, 2018]

[32] EBM-PAPST, World market leader for energy saving fans and motors. 2018. http://www.ebmpapst.com/en/ [Accessed: January 4, 2018]

[33] Micropumps-High Performance Miniature Pumps. 2018. http://www.micropumps.co.uk/ [Accessed: January 4, 2018]

[34] EOSDIS Nasa's Earth Observing System Data Information System [WWW Document]. n.d. EOSDIS NASAs Earth Obs. Syst. http://reverb.echo.nasa.gov [Accessed: July 18, 2013]

[35] Gonzalez-de-Soto M, Emmi L, Benavides C, Garcia I, Gonzalez-de-Santos P. Reducing air pollution with hybrid-powered robotic tractors for precision agriculture. Biosystems Engineering. 2016;**143**:79-94

[36] Photovoltaic Geographical Information System, JRCs Inst. Energy Transp.—PVGIS—Eur. Comm. 2018. http://re.jrc.ec.europa.eu/pvgis/ [Accessed: January 4, 2018]

[37] Labeckas G, Slavinskas S. Performance and emission characteristics of a direct injection diesel engine operating on KDV synthetic diesel fuel. Energy Conversion and Management. 2013;**66**:173-188. DOI: 10.1016/j.enconman.2012.10.004